

LAPTH-986

KEK-CP-141

KEK-TH-892

# Full $\mathcal{O}(\alpha)$ electroweak and $\mathcal{O}(\alpha_s)$ corrections to $e^+e^- \rightarrow t\bar{t}H$

G. Bélanger<sup>1)</sup>, F. Boudjema<sup>1)</sup>, J. Fujimoto<sup>2)</sup>, T. Ishikawa<sup>2)</sup>,  
T. Kaneko<sup>2)</sup>, K. Kato<sup>3)</sup>, Y. Shimizu<sup>2)</sup>, Y. Yasui<sup>2)</sup>

1) *LAPTH<sup>†</sup>, B.P.110, Annecy-le-Vieux F-74941, France.*

2) *KEK, Oho 1-1, Tsukuba, Ibaraki 305-0801, Japan.*

3) *Kogakuin University, Nishi-Shinjuku 1-24, Shinjuku, Tokyo 163-8677, Japan.*

## Abstract

We present the full  $\mathcal{O}(\alpha)$  electroweak radiative corrections to associated Higgs top pair production in  $e^+e^-$  collisions. We combine these results with a new calculation of the full one-loop QCD corrections. The computation is performed with the help of **GRACE-loop**. We find that the  $\mathcal{O}(\alpha)$  correction can be larger than the  $\mathcal{O}(\alpha_s)$  corrections around the peak of the cross section especially for a light Higgs mass. At threshold these corrections are swamped by the QCD corrections which are enhanced by the gluon Coulomb contribution. We have also subtracted the complete QED corrections and expressed the genuine weak correction both in the  $\alpha$ -scheme and the  $G_\mu$ -scheme. This reveals that the genuine weak corrections are not negligible and should be taken into account for a precision measurement of this cross section and the extraction of the Yukawa  $t\bar{t}H$  coupling.

<sup>†</sup>URA 14-36 du CNRS, associée à l'Université de Savoie.

# 1 Introduction

After the discovery of the Higgs particle at the Large Hadron Collider (LHC), one of the most pressing issue is a proper determination of the properties of this scalar since this would be an important window on the mechanism of electroweak symmetry breaking and the generation of mass. The LHC will be able to furnish a few measurements on the couplings of the Higgs to fermions and gauge bosons[1] but the most precise measurements will be performed in the clean environment of a future  $e^+e^-$  linear collider(LC)[2, 3, 4]. For example, from the measurement of the Higgs decay branching ratios, the Yukawa couplings of the light fermions can be determined at the per-cent level at a  $\sqrt{s} = 300 - 500$  GeV linear collider[2, 3, 4] if the Higgs boson has a mass below the  $W$  pair threshold. This mass range for the Higgs is consistent with the latest indirect precision data[5] and covers the range predicted for the lightest Higgs of the minimal supersymmetric model (MSSM). At a TeV scale LC, the associate production of a Higgs boson with a top quark pair,  $e^+e^- \rightarrow t\bar{t}H$ , provides a direct information on the top-Higgs Yukawa coupling. In the Standard Model,  $\mathcal{SM}$ , the cross section of the  $e^+e^- \rightarrow t\bar{t}H$  process reaches a few fb, for a light Higgs and for centre of mass energies ranging from 700 GeV to 1TeV. The expected accuracy for the determination of the top-Higgs coupling is of order 5% through the precision measurement of this process at the LC experiment[2, 3, 4, 6]. Considering such a high accuracy on the  $t\bar{t}H$  coupling one needs, on the theoretical side, to take into account the effect of radiative corrections. The purpose of this letter is to provide the full one-loop electroweak and QCD corrections to  $e^+e^- \rightarrow t\bar{t}H$  for a standard model Higgs. Preliminary results have already been presented in [7].

The full tree-level calculation of  $e^+e^- \rightarrow t\bar{t}H$  has been done a decade ago[8]. An earlier

approximate calculation had been performed by only taking into account the (dominant) photon exchange diagrams[9]. QCD radiative corrections have also been performed by two groups. Dawson and Reina investigated the  $\mathcal{O}(\alpha_s)$  corrections but only to the dominant photon exchange contribution[10]. The full  $\mathcal{O}(\alpha_s)$  correction has been computed by Dittmaier *et al.*[11]. Recently the supersymmetric QCD corrections have also been discussed in [12]. On the other hand, due to the presence of the large top Yukawa coupling, the electroweak radiative corrections may also be sizable. However, the calculation of the electroweak radiative correction has been missing. We will present new results of the full  $\mathcal{O}(\alpha)$  corrections consisting of virtual and soft corrections as well as hard photon radiation for the process  $e^+e^- \rightarrow t\bar{t}H$  in the  $\mathcal{SM}$  and will combine this result with the QCD corrections.

## 2 Grace-Loop and the calculation of $e^+e^- \rightarrow t\bar{t}H$

Our computation is performed with the help of **GRACE-loop**. This is a code for the automatic generation and calculation of the full one-loop electroweak radiative corrections in the  $\mathcal{SM}$ . It has been successfully tested for a variety of one-loop  $2 \rightarrow 2$  electroweak processes[13]. It also provided the first results on the full one-loop radiative corrections to  $e^+e^- \rightarrow \nu\bar{\nu}H$  [14, 15] which have recently been confirmed by an independent calculation[16]. For all electroweak processes we adopt the on-shell renormalisation scheme according to[13, 14, 17]. For each process some stringent consistency checks are performed. The results, for the part pertaining to the electroweak corrections, are checked by performing three kinds of tests at some random points in phase space. For these tests to be passed one works in quadruple precision. Details of how these tests are performed are given in[13, 14]. Here we only describe the main features of these tests. We first check

the ultraviolet finiteness of the results. This test applies to the whole set of the virtual one-loop diagrams. In order to conduct this test we regularise any infrared divergence by giving the photon a fictitious mass (we set this at  $\lambda = 10^{-15}\text{GeV}$ ). In the intermediate step of the symbolic calculation dealing with loop integrals (in  $n$ -dimension), we extract the regulator constant  $C_{UV} = 1/\varepsilon - \gamma_E + \log 4\pi$ ,  $n = 4 - 2\varepsilon$  and treat this as a parameter. The ultraviolet finiteness test is performed by varying the dimensional regularisation parameter  $C_{UV}$ . This parameter could then be set to 0 in further computation. The test on the infrared finiteness is performed by including both loop and bremsstrahlung contributions and checking that there is no dependence on the fictitious photon mass  $\lambda$ . An additional stability test concerns the bremsstrahlung part. It relates to the independence in the parameter  $k_c$  which is a soft photon cut parameter that separates soft photon radiation and the hard photon performed by the Monte-Carlo integration. A crucial test concerns the gauge parameter independence of the results. Gauge parameter independence of the result is performed through a set of five gauge fixing parameters. For the latter a generalised non-linear gauge fixing condition[18, 13] has been chosen.

$$\begin{aligned} \mathcal{L}_{GF} = & -\frac{1}{\xi_W} |(\partial_\mu - ie\tilde{\alpha}A_\mu - igc_W\tilde{\beta}Z_\mu)W^{\mu+} + \xi_W\frac{g}{2}(v + \tilde{\delta}H + i\tilde{\kappa}\chi_3)\chi^+|^2 \\ & -\frac{1}{2\xi_Z}(\partial.Z + \xi_Z\frac{g}{2c_W}(v + \tilde{\varepsilon}H)\chi_3)^2 - \frac{1}{2\xi_A}(\partial.A)^2 . \end{aligned} \quad (1)$$

The  $\chi$  represent the Goldstone. We take the 't Hooft-Feynman gauge with  $\xi_W = \xi_Z = \xi_A = 1$  so that no “longitudinal” term in the gauge propagators contributes. Not only this makes the expressions much simpler and avoids unnecessary large cancelations, but it also avoids the need for high tensor structures in the loop integrals. The use of the five parameters,  $\tilde{\alpha}, \tilde{\beta}, \tilde{\delta}, \tilde{\kappa}, \tilde{\varepsilon}$  is not redundant as often these parameters check complementary

sets of diagrams. Let us also point out that when performing this check we keep the full set of diagrams including couplings of the Goldstone and Higgs to the electron for example, as will be done for the process under consideration. Only at the stage of integrating over the phase space do we switch these negligible contributions.

Although the system is not fully adapted for the computation of generic QCD corrections, it is quite straightforward to implement the QCD (final state) radiative corrections to  $e^+e^- \rightarrow t\bar{t}H$ . Indeed these corrections are rather QED-like corrections. The infrared divergence can be treated by giving the gluon an infinitesimal mass while the ultraviolet divergences are treated via dimensional regularisation. Also here we adopt an on-shell scheme in particular for the top mass and wave function renormalisation. The QCD  $t\bar{t}H$  counterterm is then defined in terms of the top mass counterterm and the wave function constant. We have checked the infrared and ultraviolet finiteness of the QCD part also.

The full set of the Feynman diagrams within the non-linear gauge fixing condition consists of 12 tree-level diagrams and 2327 one-loop diagrams (with 164 pentagon diagrams) for the electroweak  $\mathcal{O}(\alpha)$  correction to the process  $e^+e^- \rightarrow t\bar{t}H$ , see Fig. 1 for a selection of these diagrams. Even though we neglect the electron-Higgs coupling, the set of diagrams still includes 6 tree-level diagrams and 758 one-loop diagrams (with 29 pentagon diagrams). We define this set as the production set. To obtain the results of the total cross sections, we use this production set. The handling of both the scalar and tensor pentagon integrals is done exactly along the lines in [14] as was used for the calculation of  $e^+e^- \rightarrow \nu\bar{\nu}H$ .

Our input parameters for the calculation of  $e^+e^- \rightarrow t\bar{t}H$  are the following. We will start by presenting the results of the electroweak corrections in terms of the fine structure constant in the Thomson limit with  $\alpha^{-1} = 137.0359895$  and the  $Z$  mass  $M_Z = 91.187$  GeV.

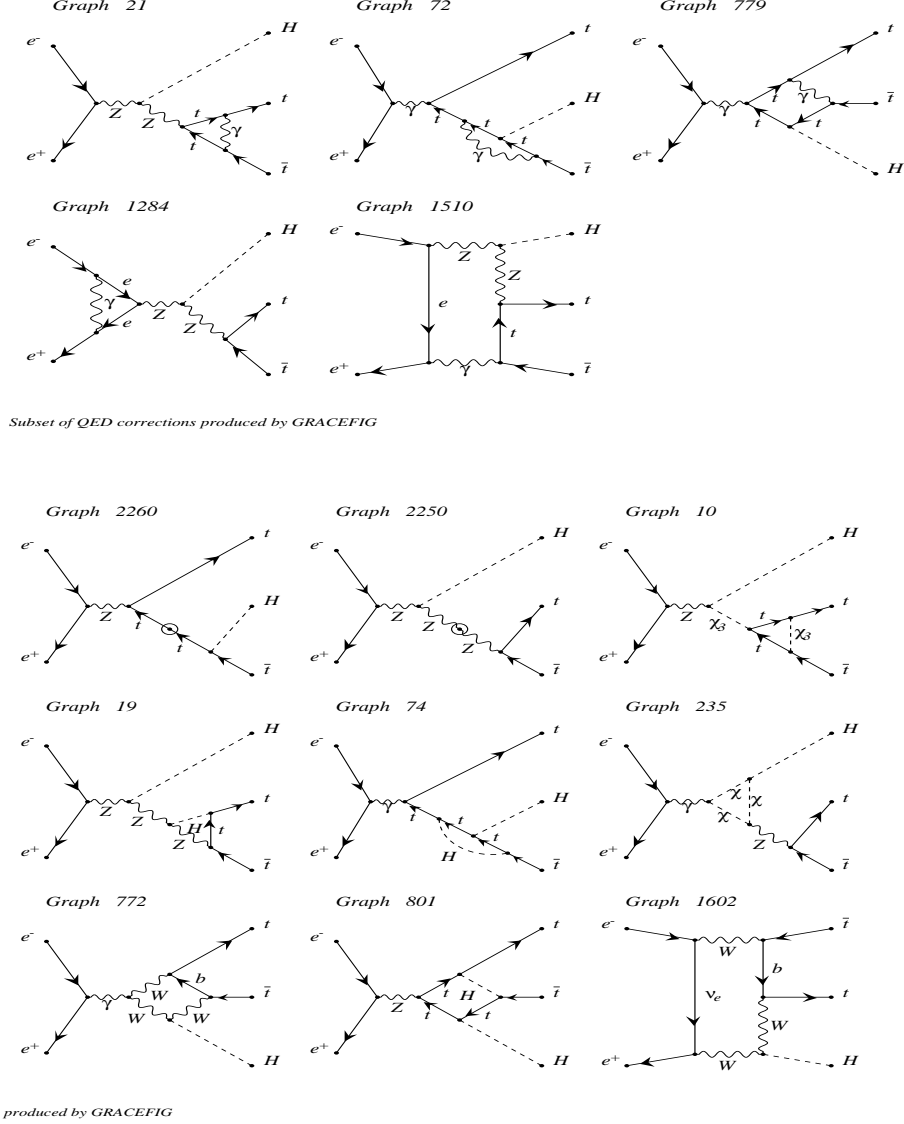


Figure 1: A small selection of different classes of loop diagrams contributing to  $e^+e^- \rightarrow t\bar{t}H$ . We keep the same graph numbering as that produced by the system. The first class of diagrams (the first 5 diagrams) are QED corrections, with the first row consisting of final state corrections. The QCD corrections diagrams can be inferred from the latter. The pentagon is a QED initial-final state interference. The second class groups genuine electroweak corrections including self-energy, triangle, box and pentagon corrections. Note that for the self-energy diagrams we collect all contributions including the counterterms in the blob. Note that the top self-energy Graph 2260 also contains a photonic correction that should be included in the first class of diagrams.

The on-shell renormalization program uses  $M_W$  as an input. However, the numerical value of  $M_W$  is derived through  $\Delta r$ [19] with  $G_\mu = 1.16639 \times 10^{-5} \text{GeV}^{-2}$ \*. Thus,  $M_W$  changes as a function of  $M_H$ . For the lepton masses we take  $m_e = 0.510999 \text{ MeV}$ ,  $m_\mu = 105.658389 \text{ MeV}$  and  $m_\tau = 1.7771 \text{ GeV}$ . For the quark masses beside the top mass  $M_t = 174 \text{ GeV}$ , we take the set  $M_u = M_d = 63 \text{ MeV}$ ,  $M_s = 92 \text{ MeV}$ ,  $M_c = 1.5 \text{ GeV}$  and  $M_b = 4.7 \text{ GeV}$ . With this we find, for example, that  $M_W = 80.3759 \text{ GeV}$  for  $M_H = 120 \text{ GeV}$  and  $M_W = 80.3469 \text{ GeV}$  for  $M_H = 180 \text{ GeV}$ . For the QCD coupling, we choose  $\alpha_s(M_Z) = 0.118$  as an input and evaluate  $\alpha_s(M_t) = 0.10754$  with the next-to-next-to-leading order renormalization group equation.

As well known, from the direct experimental search of the Higgs boson at LEP2, the lower bound of the  $\mathcal{SM}$  Higgs boson mass is  $114.4 \text{ GeV}$ [21]. On the other hand, indirect study of the electroweak precision measurement suggests that the upper bound of the  $\mathcal{SM}$  Higgs mass is about  $200 \text{ GeV}$ [5]. In this paper, we therefore only consider a relatively light  $\mathcal{SM}$  Higgs boson and take the two illustrative values  $M_H = 120 \text{ GeV}$  and  $M_H = 180 \text{ GeV}$ .

Let us first present some quantitative consistency tests on our results. For the electroweak part, the ultraviolet finiteness test gives a result that is stable over 20 digits when one varies the dimensional regularisation parameter  $C_{UV}$ . As for the gauge parameter independence checks, our results are stable over 26 digits when varying any of the non-linear gauge fixing parameters. For the QED infrared finiteness test we also find results that are stable over 20 digits when varying the fictitious photon mass  $\lambda$ . As for the  $k_c$  stability test our results are consistent within a Monte-Carlo statistical error of 0.02%.

---

\*The routine we use to calculate  $\Delta r$  has been slightly modified from the one used in our previous paper on  $e^+e^- \rightarrow \nu\bar{\nu}H$  [14] to take into account the new theoretical improvements. It reproduces quite nicely the approximate formula in [20].

We also checked the tests of the stability on the ultraviolet and the infrared finiteness for the QCD calculation. The ultraviolet finiteness test gives a result that is stable over 30 digits. The sum of loop and bremsstrahlung contributions is stable over 13 digits when varying  $\lambda_g$ , the infrared gluon mass regulator.  $k_c$  independence is consistent with a Monte-Carlo statistical error of 0.2%. In addition, we reproduced the previous results of ref.[10] when setting to zero the  $Z$  exchange diagrams and also exactly reproduced the results of Dittmaier *et al.*[11] with the full  $\mathcal{O}(\alpha_s)$  calculation within the on-shell renormalization scheme.

## 3 Results

### 3.1 Full $\mathcal{O}(\alpha)$ and $\mathcal{O}(\alpha_s)$ corrections

At tree-level, for the Higgs masses we are considering, the cross section shows a steep rise just after threshold and slowly decreases past the maximum of the cross section, see Fig. 2(a). For the measurement of the  $t\bar{t}H$  coupling it is most useful to run at the maximum of the cross section. For example for  $M_H = 120\text{GeV}$  this maximum occurs around  $\sqrt{s} = 700 - 800\text{GeV}$  where the cross section is in excess of  $2fb$ , see Fig. 2(a). For a total integrated luminosity of  $1\text{ab}^{-1}$  the  $1\sigma$  statistical error corresponds to about a 2% precision. Thus the theoretical knowledge of the cross section at 0.2% is quite sufficient. It is important to keep in mind that the dominant contribution to  $e^+e^- \rightarrow t\bar{t}H$  for the energies we are considering is due to the photon exchange diagram, the  $Z$  exchange diagrams with Higgs radiation off the  $Z$  or the top is much smaller. This is especially true at threshold. For example for  $M_H = 120\text{GeV}$  and  $\sqrt{s} = 500\text{GeV}$ , the photon exchange diagram alone contributes 90% of the total cross section whereas Higgs radiation off the  $Z$  is less than 0.2%. The importance of the photon exchange contribution lessens somehow



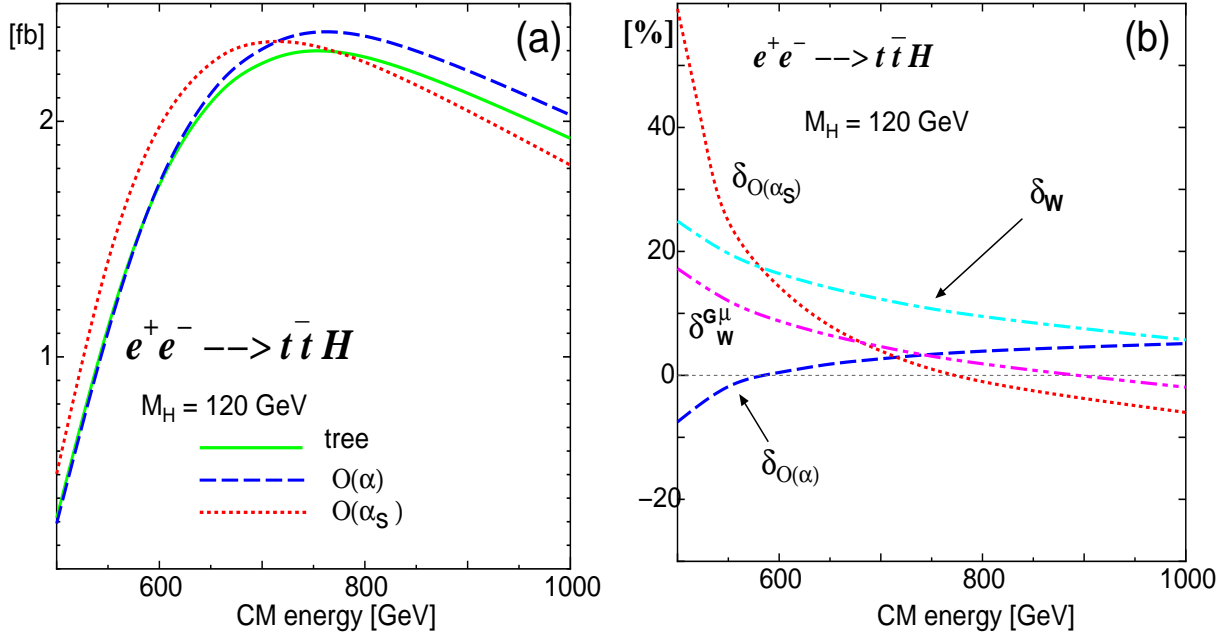


Figure 2: (a) Total cross section as a function of the centre of mass energy for  $M_H = 120$  GeV. We show the total cross sections for the tree level, full  $\mathcal{O}(\alpha)$  and  $\mathcal{O}(\alpha_s)$  level in (a). The relative corrections are shown in (b). Solid lines are tree level, dashed lines are the full  $\mathcal{O}(\alpha)$  and dotted lines are the  $\mathcal{O}(\alpha_s)$  corrections. We take  $\alpha_s(M_t) = 0.10754$ . In addition, the genuine weak correction  $\delta_W$  and the relative correction  $\delta_W^{G_\mu}$  in the  $G_\mu$  scheme are presented.

at high energies, but even at 1TeV this contribution accounts for about 80% of the total.

The full  $\mathcal{O}(\alpha)$  electroweak correction and the full  $\mathcal{O}(\alpha_s)$  QCD inclusive cross section take into account the full one-loop virtual corrections as well as the soft and hard bremsstrahlung contributions. These corrections are shown Fig. 2(a). The relative corrections defined as

$$\delta_{\mathcal{O}(\alpha, \alpha_s)} = \frac{\sigma_{\mathcal{O}(\alpha, \alpha_s)}}{\sigma_{tree}} - 1$$

are shown in Figure 2(b).

Let us first turn to the inclusive QCD correction. It is useful to write this correction as

$$\delta_{\mathcal{O}(\alpha_s)} = C_F \alpha_s(\mu) \Delta_s, \quad C_F = 4/3. \quad (2)$$

The QCD correction has a scale dependence which however, at this order, is fully contained in  $\alpha_s(\mu)$ . We will provide the exact value of  $\alpha_s(\mu)$  together with  $\delta_{\mathcal{O}(\alpha_s)}$  so that a comparison with other calculations is straightforward. As already noted in [10, 11] we confirm that the QCD corrections are quite large at threshold increasing the tree-level cross section by about 50%, for  $M_H = 120\text{GeV}$  and  $\sqrt{s} = 500\text{GeV}$ . This large increase is due essentially to the gluonic Coulomb corrections. At energies where the cross section is at its highest and the process is most likely to be of interest, the QCD corrections are quite modest. For example, for  $M_H = 120\text{GeV}$  and  $\sqrt{s} = 800\text{GeV}$ , as seen also in Table 1, the correction is a mere  $\sim -1\%$ , the residual scale dependence is very small. Indeed as shown in Table 1, the corrections for a scale  $\mu = M_t$  and  $\mu = \sqrt{s} = 800\text{GeV} \sim 4M_t$ , vary from  $-1$  to  $-0.8\%$ . A similar trend is observed for  $M_H = 180\text{GeV}$ , see Table 1. As the energy increases further past the maximum of the cross section, these corrections turn negative but remain moderate at around  $-5\%$  for  $\sqrt{s} = 1\text{TeV}$ . At these energies for the light Higgs

masses we are considering the  $M_H$  dependence of the corrections lessens.

$\sqrt{s}$	$M_H(\text{GeV})$	$\sigma_{tree}(\text{fb})$	$\sigma_{\mathcal{O}(\alpha_s(M_t))}(\text{fb})$	$\delta_{\mathcal{O}(\alpha_s(M_t))}(\%)$	$\delta_{\mathcal{O}(\alpha_s(\sqrt{s}))}(\%)$
600 GeV	120	$1.7293 \pm 0.0003$	$1.977 \pm 0.001$	14.3	12.4
	180	$0.33714 \pm 0.00004$	$0.4383 \pm 0.0004$	30.0	26.0
800 GeV	120	$2.2724 \pm 0.0005$	$2.250 \pm 0.002$	-1.0	-0.8
	180	$1.0672 \pm 0.0003$	$1.0856 \pm 0.0007$	1.7	1.4
1 TeV	120	$1.9273 \pm 0.0005$	$1.812 \pm 0.003$	-6.0	-4.9
	180	$1.1040 \pm 0.0003$	$1.049 \pm 0.001$	-5.0	-4.1

Table 1: *QCD corrections for  $e^+e^- \rightarrow t\bar{t}H$ . We also display the Monte-Carlo integration errors. We consider two different schemes. (A) We choose the renormalization scale  $\mu$  of the QCD coupling  $\alpha_s$  at  $M_t = 174 \text{ GeV}$  with  $\alpha_s(M_t) = 0.10754$ . (B) We take  $\mu = \sqrt{s}$  with  $\alpha_s = 0.09330$  at  $\sqrt{s} = 600 \text{ GeV}$ ,  $\alpha_s = 0.09051$  at  $\sqrt{s} = 800 \text{ GeV}$  and  $\alpha_s = 0.08847$  at  $\sqrt{s} = 1 \text{ TeV}$ .*

We now turn to the total  $\mathcal{O}(\alpha)$  electroweak corrections. Again taking as an example  $M_H = 120\text{GeV}$ , the  $\mathcal{O}(\alpha)$  electroweak correction is about  $-7.5\%$  around threshold at  $\sqrt{s} = 500 \text{ GeV}$  and is therefore swamped by the QCD correction. However as the energy increases, contrary to the QCD correction, the full electroweak correction slowly increases and turns positive for  $\sqrt{s} > 600 \text{ GeV}$ . Around the maximum of the cross section at  $\sqrt{s} = 800$ , the full electroweak correction is about  $+4\%$  and thus larger than the full QCD correction ( $-1\%$ ). For yet higher energies these corrections tend to cancel each other. For example for  $M_H = 120\text{GeV}$  this occurs around  $\sqrt{s} = 1\text{TeV}$ . We also show some numerical results  $M_H = 180 \text{ GeV}$  in Table 2. The  $\mathcal{O}(\alpha)$  corrections for the Higgs mass of  $180\text{GeV}$  are rather small in the range  $\sqrt{s} = 800 \text{ GeV} - 1 \text{ TeV}$ , slightly increasing from  $\sim -2\%$  to  $-0.5\%$ . In particular, for  $\sqrt{s} = 1\text{TeV}$  and  $M_H = 180\text{GeV}$  the full  $\mathcal{O}(\alpha)$ , because of its smallness, may not be resolved from the corresponding QCD corrections due to the scale dependence of the latter.

$\sqrt{s}$	$M_H(\text{GeV})$	$\sigma_{tree}(\text{fb})$	$\sigma_{\mathcal{O}(\alpha)}(\text{fb})$	$\delta_{\mathcal{O}(\alpha)}(\%)$
600 GeV	120	$1.7293 \pm 0.0003$	$1.738 \pm 0.002$	0.5
	180	$0.33714 \pm 0.00004$	$0.3126 \pm 0.0003$	-7.3
800 GeV	120	$2.2724 \pm 0.0005$	$2.362 \pm 0.004$	3.9
	180	$1.0672 \pm 0.0003$	$1.050 \pm 0.002$	-1.6
1 TeV	120	$1.9273 \pm 0.0005$	$2.027 \pm 0.004$	5.2
	180	$1.1040 \pm 0.0003$	$1.098 \pm 0.002$	-0.5

Table 2: *As in the previous table but for the total  $\mathcal{O}(\alpha)$  electroweak corrections.*

### 3.2 The genuine weak correction

In order to quantify the genuine weak corrections one needs to subtract the full QED corrections from the full  $\mathcal{O}(\alpha)$  corrections. This is important because it is well known that the QED corrections can be quite large and that in  $e^+e^-$  processes those from the initial state need to be resummed[22]. For the process at hand, which at tree-level proceeds through  $s$ -channel neutral vector bosons, these QED corrections form a gauge invariant set. This set may be further subdivided into three subsets that are also separately gauge invariant: *i*) initial state radiation, *ii*) purely final state radiation and *iii*) the initial-final state QED interference.

*i*) The dominant initial state QED virtual and soft bremsstrahlung corrections are given by the universal soft photon factor that leads to a relative correction[14]

$$\delta_{V+S,in.}^{QED} = \frac{2\alpha}{\pi} \left( (L_e - 1) \ln \frac{k_c}{E_b} + \frac{3}{4}L_e + \frac{\pi^2}{6} - 1 \right), \quad L_e = \ln(s/m_e^2). \quad (3)$$

where  $m_e$  is the electron mass,  $E_b$  the beam energy ( $s = 4E_b^2$ ) and  $k_c$  is the cut on the soft photon energy.

*ii*) The total QED final state radiation can also be read off from the result of the QCD radiative correction through the replacement  $\alpha_s(\mu) C_F \rightarrow \alpha Q_t^2$  in Eq. 2 ( $Q_t$  is the electric

charge of the top).

*iii)* The initial-final state QED correction is ultraviolet finite. Within our system this contribution can be easily isolated and combined with the appropriate bremsstrahlung counterpart leading to an infrared finite result.

Although this approach of extracting the full QED correction is the most simple one, we have also calculated the full QED corrections separately and subtracted their contributions from the full  $\mathcal{O}(\alpha)$ . In order to perform this subtraction, the QED virtual corrections are generated by dressing the tree-level diagrams with one-loop photons (the photon self-energy is not included in this class). Moreover one needs to include some counterterms. One only has to take into account the purely photonic contribution to the top mass counterterm as well as the wave function renormalisation constants of the electron and the top. Performing this more direct computation, we confirmed, that especially around threshold, to a large extent the bulk of the QED corrections originate from the initial state universal corrections. Moreover this also checked the extraction of the final QED corrections. A break up of the soft and virtual QED corrections into initial, final and interference is shown in Table 3.

We define the genuine weak relative correction as,

$$\delta_W = \delta_{\mathcal{O}(\alpha)} - \delta^{QED} = \delta_{\mathcal{O}(\alpha)} - \delta_{V+S}^{QED} - \delta_{hard}^{QED}.$$

$\delta_{V+S}^{QED}$  is the complete QED virtual and soft correction whereas  $\delta_{hard}^{QED}$  is the hard photon contribution. The weak corrections after subtraction of the QED corrections are shown in Fig. 2 for  $M_H = 120\text{GeV}$ . The total genuine weak corrections are not small, being largest around threshold ( $\sim +25\%$  at  $\sqrt{s} = 500\text{GeV}$ ) and decrease monotonically as the energy increases, see Fig. 2(b). At  $\sqrt{s} = 1\text{TeV}$  they reach about 6%. These corrections

$M_H$ (GeV)	$\sqrt{s}$ (GeV)	$\sigma_{V+S,Full}^{QED}$ ( $\sigma_{hard,Full}^{QED}$ (fb))	$\sigma_{V+S,Init.}^{QED}$ (fb)	$\sigma_{V+S,Fin.}^{QED}$ (fb)	$\sigma_{V+S,Int.}^{QED}$ (fb)	$\delta^{QED}$ (%)	$\delta_W$ (%)
120	600	-2.6092 (2.3333)	-2.557	-0.012	-0.043	-16.0	16.5
	800	-3.6667 (3.5391)	-3.516	-0.055	-0.099	-5.6	9.5
	1000	-3.2622 ( 3.2507)	-3.086	-0.071	-0.109	-0.6	5.8
180	600	-0.50490 ( 0.41839)	-0.4985	0.0056	-0.0072	-25.7	18.4
	800	-1.7120 ( 1.5975)	-1.651	-0.020	-0.043	-10.7	9.1
	1000	-1.8589 (1.8048)	-1.768	-0.035	-0.058	-4.9	4.4

Table 3: *Extraction of the QED corrections.*  $\sigma_{V+S,Full}^{QED}$  corresponds to the cross section for the full one-loop QED virtual and soft bremsstrahlung with  $k_c = 0.001 \text{ GeV}$ .  $\sigma_{V+S,Init.}^{QED}$  extracts the initial state radiation.  $\sigma_{V+S,Fin.}^{QED}$  gives the final state QED correction whereas  $\sigma_{V+S,Int.}^{QED}$  is the initial-final QED interference contribution. We also give  $\sigma_{hard,Full}^{QED}$  which is the full hard photon radiation cross section. All cross sections are in fb. We also give the relative QED correction (after including hard radiation) as well as the relative genuine weak correction as defined in the text. Note also that the extraction of the total  $\sigma_{V+S,Full}^{QED}$  and  $\sigma_{hard,Full}^{QED}$  has been computed with higher accuracy than the individual (S+V) contributions. We can check that the two computations (full) and adding the individual contributions agree.

could therefore, for this Higgs mass, always be disentangled from the QCD corrections. Past  $\sqrt{s} = 600\text{GeV}$  and up to  $\sqrt{s} = 1\text{TeV}$ , they are larger, in absolute terms, than the QCD corrections. A similar trend also occurs for  $M_H = 180\text{GeV}$ , see Table 3. For  $\sqrt{s} = 600\text{GeV}$  we find  $\delta_W \sim +18\%$  this correction drops with energy reaching  $\delta_W \sim +4\%$  at  $1\text{TeV}$  where it almost cancels the corresponding QCD correction.

Having subtracted the genuine weak corrections one could also express the corrections in the  $G_\mu$  scheme by further extracting the rather large universal weak corrections that affect two-point functions through  $\Delta r$ . This defines the genuine weak corrections in the  $G_\mu$  scheme as  $\delta_W^{G_\mu} = \delta_W - 3\Delta r$ . For reference, one has  $\Delta r = 2.55\%$  for  $M_H = 120\text{ GeV}$  and  $\Delta r = 2.70\%$  for  $M_H = 180\text{ GeV}$ . For  $e^+e^- \rightarrow \nu\bar{\nu}H$  this procedure helps absorb a large part of the weak corrections. Another advantage is that much of the (large) dependence due to the light fermions masses also drops out. For  $M_H = 120\text{GeV}$ , the relative correction  $\delta_W^{G_\mu}$  is shown as a function of energy in Fig. 2. Adopting this scheme, we find that in the energy range where the cross section is largest,  $\sqrt{s} = 700\text{GeV}$  to  $\sqrt{s} = 1\text{TeV}$ , the correction remains modest changing from about  $5\%$  to  $-2\%$ . These corrections could be “measured above” the QCD corrections. For  $M_H = 180\text{GeV}$ , the correction ranges from  $1\%$  to  $-4\%$  as the energy changes from  $800\text{GeV}$  to  $1\text{TeV}$ . However at energies around threshold, the genuine weak corrections in the  $G_\mu$  scheme are large (and positive), although about a factor 3 to 2 smaller than the QCD corrections. For  $M_H = 120\text{GeV}$  the genuine non-QED correction in the  $G_\mu$  scheme reaches  $+17\%$  at  $\sqrt{s} = 500\text{GeV}$  ( $\sim 30\text{GeV}$  above threshold). They are about  $10\%$  for  $M_H = 180\text{GeV}$   $\sqrt{s} = 600\text{GeV}$  ( $\sim 70\text{GeV}$  above threshold). These corrections slightly decrease with energy following a trend similar to the QCD corrections although the decrease is not as fast. One knows from  $e^+e^- \rightarrow t\bar{t}$  [23, 24]

that there is a Yukawa counterpart to the Coulomb large gluonic correction mediated by a Higgs exchange which is large at threshold for a large top mass and a very light Higgs mass. This phenomenon can only partially account for the large 17% increase of the cross section at  $\sqrt{s} = 500\text{GeV}$  for  $M_H = 120\text{GeV}$ , considering the value of the Higgs mass. We would like to argue that because the tree-level cross section is dominated by photon exchange, a description of the cross section in terms of  $G_\mu$  instead of  $\alpha$  may not be the most appropriate. Rather, the photon couplings should be parameterized in terms of the running  $\alpha$ . Therefore especially at threshold one should subtract from  $\delta_W$   $2\Delta\alpha(s) + \Delta r$  instead of  $3\Delta r$ . For illustration we will only use the light fermion contribution to  $\Delta\alpha(s)$ . The correction defined this way,  $\delta_{mixed} = \delta_W - 2\Delta\alpha(s) - \Delta r$ , brings down the remaining weak contribution to  $\delta_{mixed} \sim 7\%$  for  $M_H = 120\text{GeV}$  at  $\sqrt{s} = 500\text{GeV}$  and  $1.4\%$  for  $M_H = 180\text{GeV}$  at  $\sqrt{s} = 600\text{GeV}$ . For higher energies, above  $\sqrt{s} = 700\text{GeV}$ , this prescription gives large (negative) corrections. For instance, for  $\sqrt{s} = 1\text{TeV}$  we find  $\delta_{mixed} \sim -12\%$  for  $M_H = 120\text{GeV}$  and  $\delta_{mixed} \sim -14\%$  for  $M_H = 180\text{GeV}$ . Therefore none of the prescriptions,  $G_\mu$  or  $\delta_{mixed}$  reproduces the full genuine weak corrections across the whole energy range from threshold to  $1\text{TeV}$ . This should not be surprising as it has been known, already for  $2 \rightarrow 2$  processes, that the contribution of boxes becomes important as the energy increases and that the  $G_\mu$  scheme is not always the most appropriate. A case in point is  $e^+e^- \rightarrow ZH$  [25]. One may also enquire whether the leading  $m_t^2$  corrections to the  $t\bar{t}H$  coupling could account for most of the weak radiative corrections. The leading  $m_t^2$  corrections to the  $f\bar{f}H$  vertex, in the  $G_\mu$  scheme, had been worked out [26, 27]. The corrected  $t\bar{t}H$  vertex  $y_{t\bar{t}H}$  writes in terms of the tree-level one,  $y_{t\bar{t}H}^0$ , as

$$y_{t\bar{t}H} = y_{t\bar{t}H}^0 \left( 1 + \frac{7}{2} \frac{G_\mu M_t^2}{8\pi^2 \sqrt{2}} \right) \quad (4)$$



In the total cross section with  $M_t = 174\text{GeV}$  this only accounts for about 2.2% weak correction. Therefore one sees that to properly take into account the electroweak corrections to the  $e^+e^- \rightarrow t\bar{t}H$  a full calculation is needed.

## 4 Conclusions

We have performed a full one-loop correction to the process  $e^+e^- \rightarrow t\bar{t}H$  which, at a future linear collider running in the energy range 700GeV to 1TeV, can allow a direct determination of the important Yukawa coupling  $t\bar{t}H$ . The full one-loop corrections combine both the full electroweak corrections as well as the QCD corrections. Apart from the ultra-violet and infrared finiteness tests of the results, we performed, for the more involved electroweak sector, an extensive gauge parameter independence check.  $k_c$  stability has also been verified.  $k_c$  is the photon energy parameter that separates soft and hard photon (and gluon) radiation. For the electroweak part we have also extracted the contribution of the QED corrections. The final state QED correction has also been used as a further check on the QCD part. This extraction helps define the genuine weak corrections. We have expressed the latter both in the  $\alpha$ -scheme and the  $G_\mu$ -scheme. We find that, for all the Higgs masses that we have studied, the full  $\mathcal{O}(\alpha)$  corrections are swamped by the large QCD corrections at threshold. The latter can increase the cross section by as much as 50% due to the threshold Coulomb enhancement. It is interesting to note that after the extraction of the QED corrections, the genuine weak corrections at threshold are important ( $\sim 20\%$ ), although still small compared to the corresponding QCD corrections. However, around the peak of the cross section where this process is most likely to be of interest for the extraction of the Yukawa coupling, the electroweak corrections can dominate over the QCD corrections. In this energy range both corrections

are under control and for  $M_H = 120\text{GeV}$ , the genuine weak corrections expressed in the  $G_\mu$  scheme are modest ranging between 5% to -2% for  $\sqrt{s} = 500\text{GeV}$  to  $\sqrt{s} = 1\text{TeV}$ . Nonetheless they have to be taken into account for a precision analysis of this process at a future linear collider.

### Acknowledgments

This work is part of a collaboration between the **GRACE** project in the Minami-Tateya group and LAPTH. D. Perret-Gallix and Y. Kurihara deserve special thanks for their contribution. We also acknowledge useful discussions with J.P. Guillet and E. Pilon. This work was supported in part by the Japan Society for Promotion of Science under the Grant-in-Aid for scientific Research B(N°. 14340081) and PICS 397 of the French National Centre for Scientific Research (CNRS).

### Addendum

Our results for the full  $\mathcal{O}(\alpha)$  corrections were first reported in [7]. In the meantime while finalising this article there appeared a paper on the same subject[28]. These authors calculate the  $\mathcal{O}(\alpha)$  corrections using the system **FeynArts** and **FeynCalc**[29] but do not attempt to isolate the genuine weak corrections. These authors use a rather different set of input parameters. For the light quark masses they use the current quark masses which would give a much too large value of  $\Delta\alpha(M_Z^2)$ . Nonetheless taking the same input parameters we have run our program for a few points reported in[28]. With  $M_H = 115\text{GeV}$ , for both  $\sqrt{s} = 500\text{GeV}$  and  $\sqrt{s} = 1000\text{GeV}$  we find very satisfactory agreement, at least as far as one can read from their graph (Fig. 5 of [28]). We obtain  $-4.2\%$  ( $\sqrt{s} =$

500GeV) and 7.3%( $\sqrt{s} = 1\text{TeV}$ ). However for higher energies we have not been able to reproduce their results. For instance for  $\sqrt{s} = 2\text{TeV}$  we find  $\delta_{\mathcal{O}(\alpha)} \sim 8\%$  whereas they find  $\sim 4\%$ .

## References

- [1] Precision Higgs Working Group of Snowmass 2001, J. Conway *et al.*, FERMILAB-CONF-01-442, SNOWMASS-2001-P1WG2, Mar 2002. 20pp. Contributed to APS/DPF/DPB Summer Study on the Future of Particle Physics (Snowmass 2001), Snowmass, Colorado, 30 Jun - 21 Jul 2001; hep-ph/0203206.
- [2] T. Abe *et al.* [American Linear Collider Working Group Collaboration], “Linear collider physics resource book for Snowmass 2001,” in *Proc. of the APS/DPF/DPB Summer Study on the Future of Particle Physics (Snowmass 2001)* ; hep-ex/106055, hep-ex/106057, hep-ex/106058.
- [3] J. A. Aguilar-Saavedra *et al.* [ECFA/DESY LC Physics Working Group Collaboration], “TESLA Technical Design Report Part III: Physics at an e+e- Linear Collider,” arXiv:hep-ph/0106315.
- [4] K. Abe *et al.* [ACFA Linear Collider Working Group Collaboration], “Particle physics experiments at JLC,” arXiv:hep-ph/0109166.
- [5] Martin W. Grünewald, Invited talk presented at the Mini-Workshop ”Electroweak Precision Data and the Higgs Mass” DESY Zeuthen, Germany, February 28th to March 1st, 2003, hep-ex/0304023.
- [6] M. Battaglia and K. Desch, hep-ph/0101165 and references therein.

- [7] G. Bélanger, F. Boudjema, J. Fujimoto, T. Ishikawa, T. Kaneko, K. Kato, Y. Shimizu and Y. Yasui, presented at LoopFest2, Brookhaven National Laboratory, Upton, NY, May 14-16, 2003. The talk can be downloaded at this location:  
<http://quark.phy.bnl.gov/loopfest2/belanger.ps>.
- [8] A. Djouadi, J. Kalinowski and P.M. Zerwas, Z. Phys. **C54** (1992) 255.
- [9] K.J.F. Gaemers and G.J. Gounaris, Phys. Lett. **B77** (1978) 379.
- [10] S. Dawson and L. Reina, Phys.Rev.**D59** (1999) 054012.
- [11] S. Dittmaier, M. Krämer, Y. Liao, M. Spira and P.M. Zerwas, Phys.Lett. **B441** (1998) 383.
- [12] S. Zhu, hep-ph/0212273.
- [13] G. Bélanger, F. Boudjema, J. Fujimoto, T. Ishikawa, T. Kaneko, K. Kato and Y. Shimizu, in preparation.
- [14] G. Bélanger, F. Boudjema, J. Fujimoto, T. Ishikawa, T. Kaneko, K. Kato and Y. Shimizu, Phys. Lett. **B559** (2003) 252; hep-ph/0212261.
- [15] G. Bélanger, F. Boudjema, J. Fujimoto, T. Ishikawa, T. Kaneko, K. Kato and Y. Shimizu, Nucl.Phys.**B**(Proc. Suppl.) **116** (2003) 353;.
- [16] A.Denner, S.Dittmaier, M.Roth and M.M.Weber, Phys.Lett. **B560** (2003) 196; hep-ph/0301189 and Nucl.Phys. **B660** (2003)289; hep-ph/0302198.
- [17] K. Aoki, Z. Hioki, R. Kawabe, M. Konuma and T. Muta, Suppl. Prog. Theor. Phys. **73** (1982) 1.
- [18] F. Boudjema and E. Chopin, Z.Phys. **C73** (1996) 85.

- [19] We use the code from Z. Hioki, see for example Z.Hioki, Zeit. Phys. C49 (1991), 287, see also Z. Hioki, Acta Phys.Polon. **B27** (1996) 2573; hep-ph/9510269.
- [20] A. Freitas, W. Hollik, W. Walter and G. Weiglein, Nucl. Phys. **B 632** (2002) 189; hep-ph/0202131.
- [21] The LEP Higgs Working Group,  
<http://lephiggs.web.cern.ch/LEPHIGGS/www/Welcome.html>.
- [22] Y .Kurihara, J. Fujimoto, T. Munehisa and Y. Shimizu, Prog.Theor.Phys. **96** (1996) 1223.  
T. Munehisa, J. Fujimoto, Y. Kurihara and Y. Shimizu, Prog.Theor.Phys. **95** (1996) 375.
- [23] H. Inazawa and T. Morii, Phys. Lett. **B203** (1988) 279, Erratum **B207** (1988) 520.  
W. Kwong, Phys. Rev. **D43** (1991) 1488.  
M. J. Strassler and M. E. Peskin, Phys. Rev **D43** (1991) 1501.
- [24] J. Fujimoto and Y. Shimizu, *Mod. Phys. Lett.* **3A** (1988) 581.
- [25] A. Denner, J. Küblbeck, R. Mertig and M. Böhm, Z. Phys. **C56** (1992) 261.  
B.A. Kniehl, Z. Phys. C55 (1992) 605.  
See also, J. Fleischer and F. Jegerlehner, Nucl. Phys. **B216** (1983) 469.
- [26] Z. Hioki, Phys. Lett **B224** (1989) 417.
- [27] B. A. Kniehl, M. Steinhauser, Nucl. Phys. **B454** (1995) 485.
- [28] You Yu, Ma Wen-Gan, Chen Hui, Zhang Ren-You, Sun Yan-Bin and Hou Hong-Sheng, hep-ph/0306036.
- [29] T. Hahn, Comp. Phys. Commun. **140** (2001) 418.